Collision

VOLUME 14
ISSUE 1

The International Compendium for Crash Research

Vehicle Damages and Longitudinal Throwing Distances

When Using Biofidelic Dummies In Comparison To Conventional Dummies

Validation of the HAn-Brach Vehicle-ped Impact Mechanics Model

Crash-ol-o-gy

Airbag Myths, Legends & Lore

Review of Engineering Mechanics Applied to Accident Reconstruction

Parts 1-2

collisionmagazine.com

VALIDATION OF THE HAN-BRACH VEHICLE-PEDESTRIAN IMPACT MECHANICS MODEL

R. MATTHEW BRACH, DAVID FORTENBAUGH AND JON VAN POPPEL
ENGINEERING SYSTEMS INC.

Abstract

When it was introduced in 2001, the Han-Brach vehicle-pedestrian impact model was fitted to various experimental data to evaluate its performance against test data to establish the empirical parameters utilized in the model. It was also compared graphically to various data sets and other pedestrian impact models to assess the ability of the model to capture the physics of pedestrian impacts. The current research used experimental data generated at the 2017 ARC-CSI conference in Las Vegas, NV, where detailed data were collected from numerous vehicle-pedestrian impact tests, to further evaluate and validate the model. These more detailed data facilitate new comparisons of results produced by the model. The analysis showed that the Han-Brach mechanics model captured the dynamics of these experimental trials. Additional insights into the ranges of the empirical parameters used in the model were generated using these new data. In addition to the analysis using the experimental data, three examples are presented in the paper that show various applications of the Han-Brach mechanics model to reconstruct a variety of vehicle-pedestrian collisions.

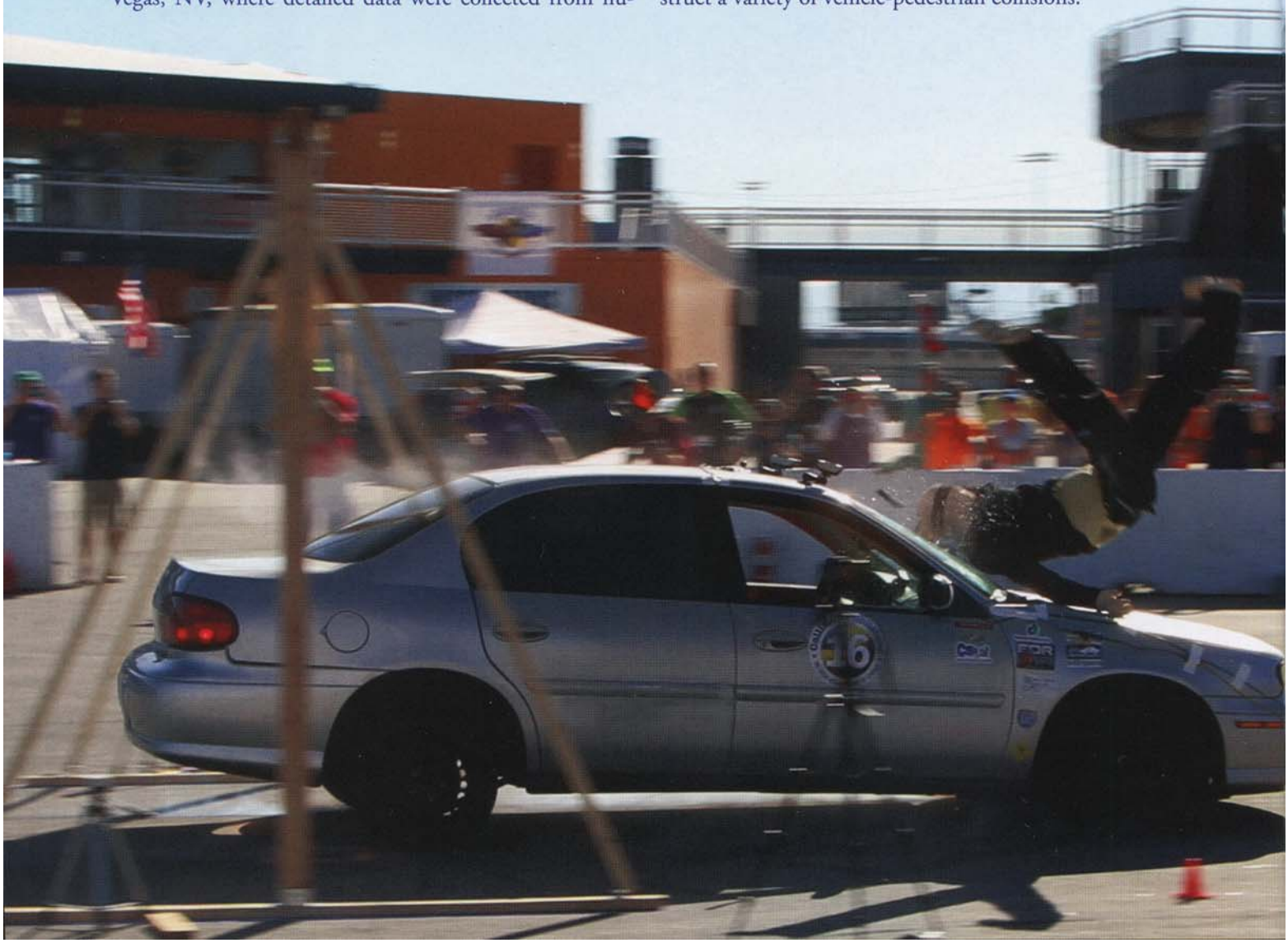

Introduction

The variety of algebraic formulas and physics models used for the reconstruction of pedestrian impacts can be separated into three categories: 1) empirical models, 2) mechanics models, and 3) multi-body modeling programs. These three categories have also been previously named as Type I, Type II and Type III, respectively.[1] Type I models are generally based on fitting a mathematical function to experimental data resulting in some form of a regression equation that relates the speed of the vehicle to the throw distance (or vice versa). Various accounts of Type I models are available in the literature.[3,4,5] Numerous Type I models were compiled into a software application.[6] Type II models are based on the principles of engineering mechanics including impulse-momentum and rectilinear motion. These models also relate the speed of the vehicle to the throw distance of the pedestrian (or vice versa). Type III models are also based on principles of mechanics, but these models treat the pedestrian as a multibody system and allow for the geometry of the vehicle that interacts with the pedestrian to be explicitly modeled with high fidelity.[15] These models may also incorporate finite element methods. Numerous publications exist for each of these three categories and deal with one or more of the generally recognized pedestrian impact configurations: wrap, forward projection, fender vault, roof vault, and somersault.[2]

The introduction of Type III models is more recent and, due to the complexity of the models, is largely based in dedicated, commercially available software that runs the models. The three most common software programs in the field of crash reconstruction that include these models are MADYMO,[7] PC-Crash [8] and HVE.[9] Various publications dealing with these programs present the theory behind the models and explore the applicability and validity of these programs.[10,11,12,13] Some publications take a broader approach and assess all three types of vehicle-pedestrian accident reconstruction methods.[14,15] One paper considers the use of a Type II model to evaluate the results of analysis done using a Type III model.[1]

The research presented here focuses specifically on the development of the Type II models (mechanics models) used for the reconstruction of vehicle-pedestrian crashes and the validation and use of one of the models specifically (Han-Brach).[19] The focus on mechanics models is motivated by a need for a useful method for reconstructing vehicle-pedestrian crashes that incorporates variables and parameters that accommodate the range of physical evidence available after a crash. For example, if the longitudinal ΔV of a vehicle involved in a crash with a pedestrian were known from imaging the event data recorder (EDR) post-crash, this physical evidence cannot be used with empirical models as empirical models do not contain this parameter. Type III multi-body models can incorporate these data, but these tools generally require considerable training and practice to master, and in some cases, significant expense. These Type III models are particularly useful when the motion of the pedestrian (arms, torso, head, etc.) or the interactions between the pedestrian and the vehicle (i.e. hood and/or windshield deformation) need to be analyzed.

Vehicle-Pedestrian Mechanics Models

Examination of the literature associated with mechanics models for vehicle-pedestrian collisions shows that one of the first publications that presented this topic was the section on pedestrian throw in the book by Collins.[16] In this treatment, Collins presented an equation for the throw distance with two components: one component related to the horizontal distance traveled during the airborne trajectory and a second equation for the travel of the pedestrian along the roadway prior to coming to rest. The next paper that tackled this topic was written by John Searle and Angela Searle.[17] In that paper, the authors presented a theory for the total trajectory of the pedestrian from impact to rest. The equation presented there provides the speed of the vehicle at impact as a function of the throw distance. The equation is:

$$V = \frac{\sqrt{2\mu g s}}{(cos\theta + \mu sin\theta)} \qquad (1)$$

In this equation, μ is the frictional drag coefficient between the pedestrian and the roadway, S is the throw distance (the total travel distance of the pedestrian from impact to rest), V is the initial velocity of the pedestrian at separation from the vehicle, and θ is the launch angle of the pedestrian relative to the roadway. In the derivation, the height of the center of mass of the pedestrian at impact is assumed to be level with the roadway. In this equation, the value μ applies to the total throw distance, not just the portion of the throw distance in which the pedestrian is engaging the roadway. In a later paper,[18] Searle presented the derivation of an alternative formula that also relates the vehicle speed to the throw distance

of a pedestrian. In this approach, the change in height of the center of mass of the pedestrian from the time of impact to the time at rest was included. This alternative formula is:

$$V = \frac{\sqrt{2\mu g(S+\mu H)}}{(cos\theta+\mu sin\theta)} \quad (2)$$

In this equation, μ is the frictional drag coefficient between the pedestrian and the roadway, θ is launch angle of the pedestrian relative to the roadway, S is the throw distance, V is the initial velocity of the pedestrian and H is the change in height of the center of mass of the pedestrian from launch to impact with the roadway (H is positive for an increase in height). In this equation, the value μ again applies to the total throw distance, not just the portion of the throw distance in which the pedestrian is engaging the roadway.

Another paper that considers the pedestrian throw problem from the perspective of classic kinematic equations is Aronberg.[26] He presents a detailed analysis of the general problem of the throw distance incorporating arbitrary CG height at launch and explicitly including the apogee of the postimpact flight of the pedestrian in the equations. This development addresses the kinematics of the pedestrian but does not include analysis of the impact between the vehicle and the pedestrian or the impact between the pedestrian and the roadway. In a subsequent paper,[28] the author considers the impact between the pedestrian and the roadway including a description of testing that shows the impact with the ground does affect the stopping distance of the pedestrian. The results of that testing validate the need for a Type II pedestrian throw model to include the impact between the pedestrian and the roadway in the model.

The Han-Brach Mechanics Model

The Han-Brach vehicle-pedestrian impact model,[19] introduced in 2001 and built on the previous Type II models, provides the means to analyze and reconstruct vehicle-pedestrian crashes using the principals of Newtonian mechanics. The model provides an approach different from the numerous empirical models that have been the mainstay of vehicle-pedestrian impact analysis and reconstruction for the last three decades of the 20th century. These empirical models were based on experimental data and generally provided an algebraic relationship between the measured speed of the vehicle at impact and the resulting measured throw distance of the pedestrian. Thus, these empirical models did not involve the specifics of the collision to be reconstructed (vehicle mass, etc.) or any of the physical evidence generated during the investigation other than the throw distance itself (which is frequently unknown). Consequently, these Type I empirical models offered no means to utilize any available physical evidence in the reconstruction of a crash. Type II mechanics models provide this capability.

In the original publication, the Han-Brach mechanics model was fitted to the experimental data available at the time to establish the values and ranges of the various parameters utilized in the model and to assess the overall agreement between the model and the data. The result of this fitting process, with the appropriate ranges of empirical parameters determined in the analysis, showed that the model agreed reasonably well with the data. However, the experimental data used in the analysis, the best available at that time, were quite general. These data provided essentially only the speed of the vehicle and the throw distance and generally did not include parameters such as the mass of the test vehicle and the pedestrian dummy, roadway-vehicle and roadway-pedestrian drag factors, etc. These, and other quantitative parameters, are integral to the mechanics model. A distinct advantage of a Type II model that includes these parameters is in the evaluation of the uncertainty of a crash reconstruction. The uncertainty of the result of a reconstruction due to the variation in a given parameter can only be evaluated if the model incorporates that parameter. This is a very important consideration of the selection of a model for reconstructing a pedestrian crash.

For example, the uncertainty of the reconstructed preimpact speed of a vehicle due to the variation of the frictional drag between the pedestrian and the roadway (perhaps using a high-low calculation approach) can be evaluated only if the frictional drag is a parameter in the model. For the case of any of the Type I models, the value of frictional drag does not appear, so the uncertainty of those empirical models to that parameter cannot be calculated. It is very important to point out that the confidence intervals that are typically provided as part of the empirical models (the 85th percentile confidence intervals, for example) do not quantify the uncertainty for a particular crash reconstruction. These bounds associated with a given set of experimental data quantify the uncertainty of the data from all the tests in the compilation. For example, variation is introduced into the resulting data in that the masses of the different vehicles used in the tests, which were generally not recorded as they do not appear in the model, results in uncertainty in the throw distances. In aggregate, the uncertainty quantified by the percentile bounds is not the uncertainty of any given reconstruction or trial but rather the quantification of the uncertainties of all the trials in the population that were run. This uncertainty comes from the

variety of vehicles that were used in the tests, the variety of manikins that were used in the tests, the different clothing on the manikins, the different roadway surfaces, etc. These uncertainties are independent of, and do not apply to, the uncertainties of a specific crash that is being reconstructed.

It might be argued that the uncertainty captured by the confidence intervals in a Type I model likely provides reasonable bounds for the reconstruction of any particular crash. Supporting that argument is the large range of throw distance captured by the intervals. For example, in one plot of experimental data of over 90 tests [3] the range of the 85th percentile bands is approximately ±10 kph (±6.2 mph). It may be for some reconstruction applications this range is acceptable; in other applications it may not be acceptable.

The analysis presented here utilized more complete data sets that included the details needed for direct comparison between the Han-Brach Type II mechanics model and a given test. For example, the data collected during the tests included here utilized, among other measurements, video of the impact and the post-impact trajectory of the manikin and the vehicle. The video allowed for analysis of the times associated with the various phases of the test. This level of detail was never available in prior data. Additional measurements collected during the testing were the throw distances, the pre-impact speeds of the vehicles, the accurate masses of the manikins and the vehicles at the time of the test, and the heights of the centers of mass of the manikins, among other parameters. Some parameters were estimated from the video, including the flight distance of the manikin and the distance the vehicle moved during the contact interaction with the manikin.

The Vehicle-Pedestrian Impact (Type II) Mechanics Model

Figure 1 shows various vehicle and pedestrian positions corresponding to a **wrap** vehicle-pedestrian event. Also included are the various physical distances and some other physical parameters that are associated with the postimpact motion of the vehicle and the pedestrian. Initial contact between the front of the vehicle and the pedestrian occurs at time $\tau = 0$ with the velocity of the vehicle of v_{c0}. The vehicle and pedestrian move forward at different speeds until time, $\tau = \tau_0$, when a secondary impact between the torso (and possibly the head) of the pedestrian and the hood of the vehicle occurs. Between $\tau = 0$ and $\tau = \tau_0$, the center of gravity of the pedestrian has moved forward a distance x_L and is at a height, h, above the ground as shown in the diagram. As the diagram implies, the derivation of the model equations is made with the assumption that the postimpact motions of both the vehicle and the pedestrian lie in the same geometric plane in which the x-axis lies along the heading of the vehicle and the y-axis is perpendicular to the roadway. In general, this assumption is reasonably met in actual collisions. The motion of the pedestrian is modeled as a point mass, i.e. the rotational inertia considerations of the torso and/or appendages is neglected. Additionally, any aerodynamic effects of the flight of the pedestrian are neglected.

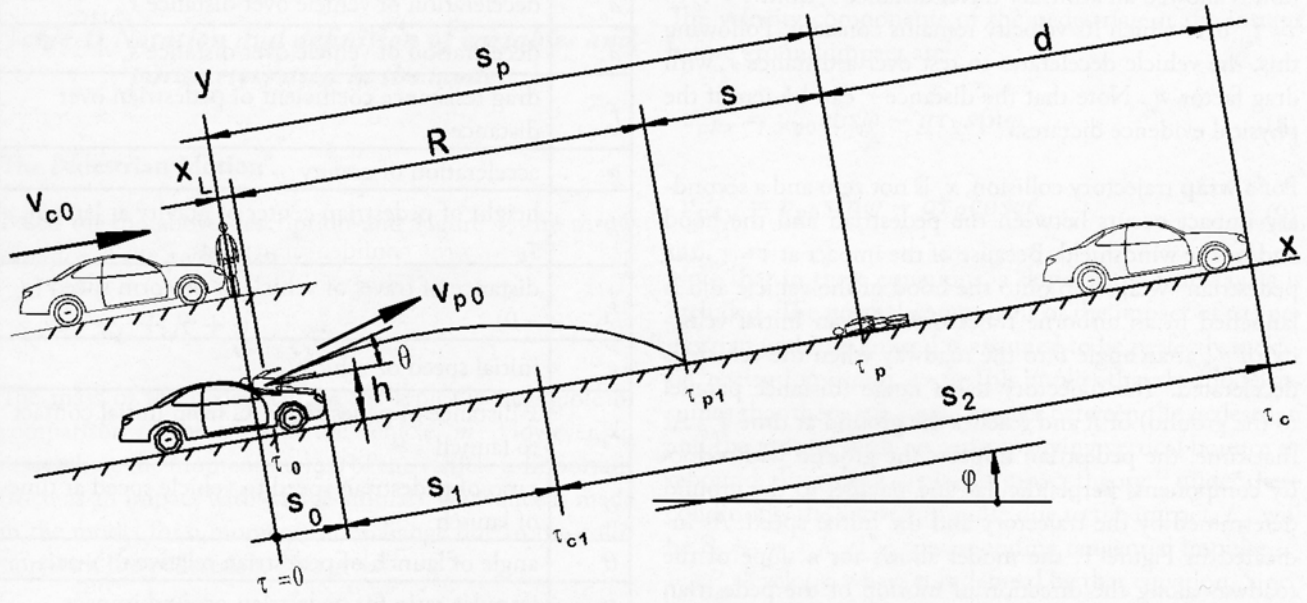

Figure 1: Diagram showing coordinates and variables associated with the Han-Brach vehicle-pedestrian Type II collision model

For a **forward projection** collision, the user-specified value of x_L is zero and there is no secondary impact between the pedestrian and the vehicle. Because of the impact, the pedestrian is projected forward instantaneously and is launched in an airborne trajectory with a velocity of v_{p0} and at an angle θ. In general, for a forward projection collision, the initial angle of motion of the pedestrian is parallel to the road, i.e. $\theta = 0°$. The trajectory of the pedestrian has a range (the distance parallel to the ground) of R and reaches the ground at time τ_{p1}. At that time, the pedestrian impacts the ground with velocity components parallel and perpendicular to the ground determined by the trajectory and the initial speed. Due to the impact with the roadway, the pedestrian undergoes a change in speed (ΔV) that has two components, one along the roadway (the x-axis) and another perpendicular to the roadway (the y-axis).

From the location of the center of gravity (CG) of the pedestrian at the time of the ground impact to the location of the CG of the pedestrian at rest, a distance s, the pedestrian is assumed to be uniformly decelerated with a sliding frictional drag factor, f_p. The motion of the pedestrian over the distance s typically consists of a combination of rolling, sliding and tumbling. It is assumed that this motion does not include any impacts with other environmental features (such as a curb, a tree or any other vehicle). The total travel distance of the pedestrian from initial contact with the vehicle to rest is the throw distance, s_p. It is assumed that from the time of separation of the pedestrian from the vehicle to the time of rest, τ_p, the pedestrian motion is completely independent of the vehicle. To provide a degree of generality for reconstructions, the vehicle motion is allowed an arbitrary travel distance s_1 from $\tau = \tau_0$ to $\tau = \tau_{c1}$ over which its velocity remains constant. Following this, the vehicle decelerates to rest over a distance s_2 with drag factor, a_0. Note that the distance s_1 can be zero if the physical evidence dictates.

For a **wrap** trajectory collision, x_L is not zero and a secondary impact occurs between the pedestrian and the hood and/or the windshield. Because of the impact at $\tau = \tau_0$, the pedestrian "wraps" up onto the hood of the vehicle and is launched in an airborne trajectory with an initial velocity of v_{p0} at an angle θ to the roadway when the vehicle is decelerated. The trajectory has a range (distance parallel to the ground) of R and reaches the ground at time τ_{p1}. At that time, the pedestrian impacts the ground with velocity components perpendicular and parallel to the ground determined by the trajectory and the initial speed. As indicated in Figure 1, the model allows for a slope of the roadway along the direction of motion of the pedestrian and the vehicle. This slope is shown as φ and is assumed to be the same for the vehicle and the pedestrian over the respective ranges of motion.

Due to the impact with the roadway, the pedestrian undergoes a sudden change in speed that has two components, one along the roadway (the x-axis) and another perpendicular to the roadway (the y-axis). From the point of ground impact to the point of rest, a distance s, the pedestrian is assumed to be uniformly decelerated with an initial speed following the impact with the roadway (and the associated ΔV) and a frictional drag factor, f_p. The motion of the pedestrian over the distance s typically consists of rolling, sliding and tumbling. The total travel distance of the pedestrian from initial impact to rest is the throw distance, s_p. It is assumed that from the time of separation, τ_0, to the time of rest, τ_p, the pedestrian motion is independent of the motion of the vehicle. For wrap collisions, the vehicle can be decelerated over the distance s_0 at a constant deceleration of $-a_0$, and then over the distance s_2 with a constant deceleration of $-a_0$. Allowing a_0 and a_2 to be different creates flexibility in the model, but generally these values are the same. For $a_0 \neq 0$ and $a_2 \neq 0$, the vehicle will decelerate from the time of initial contact with the pedestrian to rest. Under these circumstances, the distance s_1 is necessarily zero. Following separation, the vehicle decelerates to rest over a distance s_2 with constant deceleration, $-a_0$. With this information, equations can be derived to develop a Type II mechanics/analysis model. Table 1 lists the notation and definition of each of the variables used in the model.

Input Parameters	
a_0	deceleration of vehicle over distance s_0
a_0	deceleration of vehicle over distance s_2
f_p	drag resistance coefficient of pedestrian over distance s
g	acceleration of gravity
h	height of pedestrian center of gravity at launch, τ_0
s_1	distance of travel of vehicle at uniform speed ($a_0 = 0$)
v_{c0}	initial speed of vehicle
x_L	x-distance of pedestrian CG from initial contact to launch
α	ratio of pedestrian speed to vehicle speed at time of launch
θ	angle of launch of pedestrian relative to x-axis
μ	impulse ratio for pedestrian-ground impact
φ	road grade angle (positive value for uphill)

m_c	mass of vehicle, weight /g
m_p	mass of pedestrian, weight /g
s_0	distance of travel of vehicle during pedestrian contact
Output Parameters	
v'_{c0}	velocity of vehicle after impact with pedestrian
v_{p0}	initial speed of pedestrian following separation from the vehicle
R	range of pedestrian throw, launch to ground impact
τ_{p1}	time from impact to pedestrian initial contact with ground
s	pedestrian ground contact distance, impact to rest
s_p	pedestrian throw distance; total distance, initial contact to rest
τ_p	total time of travel of pedestrian, initial contact to rest
τ_{c1}	time of travel of vehicle at steady speed
s_2	distance of travel of vehicle with uniform deceleration, a_0
τ_c	vehicle travel time, initial contact to rest
d	distance between rest positions of vehicle and pedestrian
t_0	time of travel of the vehicle over s_0 with uniform deceleration, a_0

Table 1: Notation and definition of variables and parameters used in the model

The Pedestrian Motion

Based on the above description and Figure 1, the throw distance of the pedestrian is:

$$s_p = x_L + R + s \tag{3}$$

The mass of the pedestrian, m_p, is typically negligible in comparison to the mass of the vehicle, m_c. However, in cases where the momentum loss of the vehicle is important (such as an impact with a large animal), allowance is made in the model for a momentum exchange due to the collision with the pedestrian. This gives:

$$v'_{c0} = \frac{m_c}{m_c+m_p} v_{c0} \tag{4}$$

From the momentum exchange, the change in speed of the vehicle is calculated. This allows for the use of ΔV data from an EDR if data are imaged from the vehicle or an appropriate threshold is available.

For generality in the model, a factor, α, is introduced that relates the initial pedestrian velocity to the velocity of the vehicle such that:

$$v_{p0} = \alpha v'_{c0} \tag{5}$$

The parameter α is an empirical parameter that can be determined from the data. It is assumed that aerodynamic drag acting on the pedestrian is negligible as the pedestrian undergoes the motion through the air over the range R. Under such a condition, the trajectory of the CG of the pedestrian is parabolic with zero horizontal acceleration and uniform vertical acceleration due to gravity. This leads to the following equations for the range, R, and trajectory time, τ_R:

$$R = v_{p0}cos\theta\tau_R - \frac{1}{2}gsin\varphi\tau_R^2 \tag{6}$$

and

$$\tau_R = \frac{v_{p0}sin\theta}{gcos\varphi} + \frac{\sqrt{v_{p0}^2 sin^2\theta + 2ghcos\varphi}}{gcos\varphi} \tag{7}$$

The velocity components of the pedestrian at the instant before ground impact are:

$$v_{pRx} = v_{p0}cos\varphi - g\tau_R sin\varphi \tag{8}$$

$$v_{pRy} = v_{p0}sin\varphi - g\tau_R cos\varphi \tag{9}$$

Note that in these equations, a slope of the roadway, φ is included. The normal component of the impact of the pedestrian with the ground is assumed to be perfectly inelastic, restitution is zero, $e = 0$. This implies that the model assumes that there is a single impact between the pedestrian and the ground with no accompanying vertical bounce or rebound. According to planar impact theory [22] under these conditions, the vertical impulse due to the impact, P_n, will be $P_n = -m_p v_{pRy}$. The corresponding tangential impulse, $P_t = \mu P_n$ develops, where μ is defined by that equation. Since it is assumed that the interaction between the roadway and the pedestrian throughout the ground impact is sliding,

tumbling and/or rolling (no multiple impacts, or bouncing), $\mu = -f_p$. This leads to a velocity at the beginning of the slide distance, s, of:

$$v'_{pRx} = v_{pRx} + \mu v_{pRy} \quad (10)$$

The source of this equation has not been previously shown and is provided in Appendix A for completeness.

With this speed of the pedestrian at the start of the tumble/sliding phase, the tumble/slide distance s can be calculated using the following equation for uniform deceleration:

$$s = \frac{(v'_{pRx})^2}{2g(f_p cos\varphi + sin\varphi)} \quad (11)$$

Vehicle Motion

Following the change in momentum of the vehicle due to impact with the pedestrian, the motions of the vehicle and pedestrian are assumed to be independent of each other after separation, $\tau > \tau_0$. Any incidental contact during the early part of the trajectory as the pedestrian is wrapping up onto, or separating from, the hood and windshield or secondary interaction(s) with the hood as the pedestrian is falling back to the roadway, is neglected. Over the distance, s_0, and time, τ_0, the initial speed of the vehicle is v_{c0}, and the vehicle decelerates uniformly at a deceleration of a_0 (which can be zero). Over the distance s_1 and time interval ($\tau_{c1} - \tau_0$), the vehicle travels with the speed at the end of the distance s_0 with no deceleration. The distance s_0 can also be zero. Uniform deceleration of a_0, occurs over the distance s_2. The difference between the total travel distance of the vehicle and the pedestrian throw distance is labeled as the variable d. This distance is given by the following equation: $d = s_0 + s_1 + s_2 - s_p$. The default sign convention is that d is positive for the vehicle traveling further than the pedestrian. Correspondingly, d will be negative if the pedestrian travels farther then the vehicle.

Note that the model as presented above contains capability that was not part of the model as presented initially in 2001.[19] This new version of the model allows for the vehicle to decelerate over the distance s_0 with deceleration a_0. This allows for the vehicle to decelerate over the entire distance from initial contact with the pedestrian at $\tau = 0$ to rest if the physical evidence supports this characterization of the events. The previous edition of the model did not provide this capability. This additional capability permits brake application during the momentum exchange. This feature unfortunately confounds the speed change due to the momentum exchange with the speed change due to the braking.

The distance between the rest positions of the pedestrian and the vehicle can be important in a speed reconstruction of a vehicle-pedestrian impact. After an incident, the location of the pedestrian at the onset of contact between the vehicle and the pedestrian is often unknown (determining the pedestrian location at impact might actually be the goal of the reconstruction). However, the distance d may be known since the rest positions of the vehicle and the pedestrian may be known from measurements or can be reasonably estimated from the scene photographs. In such cases, it is sometimes possible to reconstruct the vehicle preimpact speed and the impact location using the distance d. This technique using a Type II model is discussed elsewhere.[20,21]

In summary, the assumptions under which the model is derived are:

1. The model assumes that the motion of the vehicle and the pedestrian occurs in the XZ plane, i.e. there is negligible transverse (lateral) motion of the pedestrian and/or the vehicle.

2. The preimpact speed of the pedestrian is such that assumption 1) is met.

3. Point mass impact (no rotational inertia is considered) is used to model the impact between the vehicle and the pedestrian and the vehicle and the pedestrian interact once (e.g. the vehicle does not roll over the pedestrian following the initial impact).

4. No rigid body (rotational) motion of the pedestrian is incorporated into the impact between the pedestrian and the ground.

5. None of the properties or dimensions of the vehicle, other than the mass, are explicitly used in the model although this factors into whether the interaction is categorized as a wrap trajectory of frontal projection.

6. The ground motion of the pedestrian consists of a single initial impact with an accompanying ΔV (with components along and perpendicular to the road) followed by uniform deceleration during which the pedestrian is sliding, tumbling, etc.

7. The throw model of the pedestrian (postimpact) does not permit multiple impacts (such as impacts of the pedestrian with curbs, poles, parked vehicles, or other objects).

8. Aerodynamic loading of the pedestrian during flight is not included in the model.

9. Application of the method to wrap and forward projection collisions has been validated using experimental data; reconstruction of roof vaults and somersault crashes is possible but no data is available for validation; the model does not handle crashes where the pedestrian is carried by the vehicle or for fender vaults. Fender vaults have been considered elsewhere.[23]

Analysis Based On Experimental Data

A series of vehicle-pedestrian impact tests were conducted in September 2017 in Las Vegas, NV under the auspices of the ARC-CSI. These tests involved a variety of different light vehicles (sedans to full size vans) and a variety of different pedestrian manikins. Some of the tests involved a single vehicle striking two manikins. Some of the manikins were specifically fabricated to be lighter than the corresponding human counterpart to study the effects of pedestrian mass on the motion of the pedestrian (this topic is not studied here). Additionally, only tests involving manikins with realistic properties (dimensions, weights, etc.) were considered in the analysis here. Data from two "forward projections" and six "wrap trajectories" were used to study the Han-Brach mechanics model with the intent of assessing the ability of the model to 1) capture the dynamics of the pedestrian crash tests and, 2) establish ranges of the empirical parameters in the model (f_p, α, θ and μ). Consistent with the nature of the model, this assessment included the impact and the motions of the pedestrian and the vehicle following separation.

For the current testing and analysis, the input variables of the Han-Brach model were generally divided into three categories. Some variables were directly measured prior to or during the trial (e.g. m_c, m_p, and v_{c0}), some variables were estimated based on video review (e.g. h, x_L, and s_0), and some variables were allowed to vary with upper-bound and lower-bound constraints and ultimately determined using Microsoft Excel's Solver utility using a best fit procedure (e.g. a_0, f_p, α, θ and μ). The deceleration of the vehicle, a_0, was constrained between 0.5 g and 0.9 g, and the pedestrian/road drag coefficient, f_p, and impulse ratio of the pedestrian/road impact, μ, were both constrained between 0.3 and 1.0. Two additional variables had unique constraints based on the collision type. For "forward projections," θ was assumed to be zero (i.e. the pedestrian center of mass is launched parallel to the roadway), and α was allowed to vary but constrained between 1.0 and 1.3 based on the original Han-Brach work.[19] For "wrap" trajectories, α was assumed to be 1.0 (i.e. no "rebound effect"), and θ was allowed to vary but constrained to a range based on video review. It was also assumed that a_0 was equal to $-a_0$ (i.e. deceleration of the vehicle throughout braking at a constant level) as this was the intent of the driver in each trial and was verified for each trial with observation of the video. Thus, s_1 was set equal to zero in all analyses. Additionally, the asphalt skid pad where the testing was conducted was essentially flat and level, so in all cases φ was set to zero.

To further guide the results based on the experimental data, some of the output variables of the Han-Brach model were also constrained and/or ultimately entered as parameters for which they could be solved. Based on video review, R was constrained within an appropriate 10 - 15 foot window. While it may seem counterintuitive that the value of R would not be uniquely determined for a given test using the video of the event, it was typical with all the trials that initial contact with the roadway after separation with the vehicle might occur in stages/phases. The first contact might involve one of the hands, then followed by a foot, before perhaps a hip (or some other part of the torso) contacts the ground. The main point here is that the model assumes that the impact of the pedestrian with the roadway occurs instantaneously in a singular location (thus defining R), whereas in the tests, which involve a dummy/manikin with articulated appendages, this interaction generally did not happen instantaneously. Thus, the model approximates this interaction.

The purpose of the Solver algorithm was to use the equations of the Han-Brach model to minimize a single value, Q, referred to as the quality function. The quality function, Q, is the sum of squares of the differences between the directly measured/assessed values of selected parameters and the model's estimates (calculations) of these same parameters. The general form of the quality function, Q, used in the analysis is shown in Equation 12. With this minimization approach, the resulting fit between the model and the data is a "best fit" in the least squares sense.

$$Q = \sum_{i=1}^{n} w_i \, (u_i - u_i^{data})^2 \qquad (12)$$

In this equation, n is the number of parameters to be used from the test data, w_i is a weighting factor (which may be 1), u_i is the parameter calculated using the pedestrian impact model and u_i^{data} is the corresponding value of the parameter determined from test measurements.

Review of the data available from the tests shows that many of the variables and parameters in the model (see Table 1) have corresponding experimental values and thus could be included in the fitting process as a term in the quality function. The general scheme associated with the analysis is to use the data acquired during testing to determine the input

parameters that were not directly measurable (although perhaps can be bounded in the analysis).

The selection of the variables used for the quality function was based primarily on the level of uncertainty associated with the determination of the value. Values of parameters such as R and τ_{p1} had considerable uncertainty and were deemed by the authors to be poor candidates for use in the quality function whereas values such as the distance the pedestrian moved from initial contact to rest, s_p, and the time associated with this motion, τ_p, were physically measured post-crash (s_p) or determined from the video (τ_p) with high accuracy and precision. These latter two parameters were deemed by the authors as good parameters for use in the quality function. Based on this rationale, four parameters were selected for use in the quality function in the analysis presented here. These four parameters were: s_p, $s_0 + s_1 + s_2$, τ_c, and τ_p.

The authors recognize that the use of the quality function with values of the u_i^{data} that are of different magnitudes can produce a fit that may better satisfy the values of larger magnitude. This disparity in the fitting can be mitigated by weighting factors. In the case of the selection of two times and two distances for the quality function used here, the distances have a magnitude that is roughly 10 times that of the value of the times used in the function. Thus, the value of the weighting, w_i, of the time values (see Equation 12) were weighted by ten in the calculation of Q whereas the weighting of the distances was one. These weighting assignments were used throughout all the analyses.

Results

Wrap Collisions

The pedestrian throw distances (s_p) and times (τ_p) calculated by the model for all the trials were all exact matches with the experimental data. The vehicle distances ($s_0 + s_1 + s_2$) calculated by the model for all the trials were within one foot of the measured experimental data, and the calculated vehicle travel times (τ_c) were within 0.16 seconds of the measured values. The vehicle deceleration values (a_0) generated through the model ranged between 0.64 and 0.75 g's, the drag coefficients between the pedestrian and the roadway (f_p) ranged between 0.38 and 0.66, and the impulse ratio (μ) ranged between 0.59 and 1.00. The launch angles (θ) ranged between 5° and 25°. The Q values for the six wrap impacts ranged between 0.59 and 3.01, considered good agreement between the Han-Brach model and the experimental data.

Forward Projections

Like the wrap collisions, the pedestrian distances (s_p) and times (τ_p) calculated by the model were exact matches, the vehicle distances ($s_0 + s_1 + s_2$) calculated by the model were within one foot of the measured experimental data, and the calculated vehicle travel times (τ_c) were within 0.06 seconds of the measured values. The vehicle deceleration values (a_0) generated through the model were 0.69 g and 0.71 g, the drag coefficients between the pedestrian and the roadway (f_p) were 0.49 and 0.64, and the impulse ratios (μ) were 0.79 and 0.80. The rebound coefficients (α) were 1.15 and 1.28. The Q values for the two forward projection impacts were 0.04 and 0.51, indicating good agreement between the Han-Brach model and the experimental data.

Comments on the values and ranges of the parameters resulting from the analysis are provided in the Discussion section following three example reconstructions. Table B.1 in Appendix B contains the numerical results of the analysis of each of the eight experimental trials analyzed.

Example Pedestrian Crash Reconstructions

Three examples are presented that show the use of the Han-Brach Type II pedestrian throw model. The first example reconstruction shows the utility of the model to reconstruct the speed of the vehicle based on the rest positions of the vehicle and the pedestrian. This approach uses the motion of both the vehicle and the pedestrian, both of which are modeled in the Han-Brach Type II pedestrian throw model, to determine the preimpact speed of the vehicle. This topic has been examined elsewhere.[21] The second example reconstruction employs the use of EDR data in the reconstruction of the crash. In this example, the determination of the speed of the vehicle at impact is not the goal as that is given by the data. Rather, it is the location of the pedestrian at the time of impact that is of interest. This location establishes whether the pedestrian was in the crosswalk. The third example is an application of the pedestrian throw model to determine the speed of a motorcycle approaching an intersection when it collides into the side of a minivan. Because of the crash, and the sudden deceleration of the motorcycle, the rider was launched into the air and over the vehicle. The rider subsequently hit the roadway and tumbled to rest. The authors are unaware of a complete treatment of the reconstruction of this type of crash using a pedestrian throw model in the literature. Prior to getting into the details of the reconstruction, the authors present the assumptions to be met for this specific use of the reconstruction model. The examples presented here were analyzed using the implementation of the Han-

Brach model with the development provided above in Equations 3 – 11.

Example 1: Pedestrian Crash Reconstruction from Rest Positions

A vehicle-pedestrian wrap collision occurs on a roadway with both the speed of the vehicle and the throw distance being unknown. The point of impact is unknown but the rest positions of the vehicle and the pedestrian are known from the scene photos. Thus, it is known that the pedestrian traveled 20 feet farther than the vehicle. Additionally, it is known that the car decelerated uniformly from before impact to rest with the driver braking heavily from impact to rest. The parameters for the reconstruction are defined as:

a_0	0.9	deceleration of vehicle over distance s_2
f_p	0.8	drag resistance coefficient of pedestrian over distance s
h	4.0 ft	height of pedestrian center of gravity at launch, t_0
s_1	0.0 ft	distance of travel of vehicle at uniform speed
x_L	2.0 ft	x-distance of pedestrian from initial contact to launch
α	1.0	ratio of pedestrian speed to vehicle speed at time of launch
θ	5.0°	angle of launch of pedestrian relative to road (x-axis)
φ	0.0°	road grade angle
μ	0.8 (= f_p)	impulse ratio for pedestrian-ground impact
m_c	93.24 lb-s^2/ft	mass of vehicle, weight/g
m_p	5.44 lb-s^2/ft	mass of pedestrian, weight/g

Using these values, the speed of the vehicle that causes the distance d (see Figure 1) to go to -20 feet can be calculated iteratively or using optimization methods. For these parameter values the speed of the vehicle is 66.6 ft/s (45 mph).

Example 2: Pedestrian Crash Reconstruction Using EDR Data

In this example, the EDR on the pickup truck was imaged shortly after the crash. Data associated with a Non-deployment event was stored in the module. Based on the key cycle count and the characteristics of the data, it was determined that the non-deployment event stored in the EDR was associated with the pedestrian impact. It is interesting to note that the collision with the pedestrian did register as a non-deployment event on this module.

Two pieces of useful information were obtained from the data: 1) the speed of the vehicle at 1 second prior to algorithm enable (AE) was 29 mph, and 2) the Maximum SDM (Sensing Diagnostic Module) Recorded Velocity Change was 1.03 mph. Additionally, the data show that the speed of the vehicle at 2 seconds before AE was also 29 mph and that the brake pedal was never applied prior to 1 second before AE. Thus, for the reconstruction, the speed of the vehicle at the time of impact with the pedestrian was taken to be 29 mph. Figure 2 is a scale diagram that shows the roadway environment where the crash occurred. The rest position of the pedestrian, as shown in the diagram, is known from measurements made by the police during their scene investigation.

The reconstruction of the location of the pedestrian relative to the crosswalk at the time of the crash is a two-step process. The first step is another level of validation of the data, and that is to assess further whether the data belong to the crash using the Maximum SDM Recorded Velocity Change. Note that this value is a function of the speed of the vehicle at the time of impact (which was extrapolated from the value recorded at -1 AE by the EDR) and the masses of the vehicle and the pedestrian. In this case, the combined weight of the vehicle and the driver was 3803 pounds and the weight of the pedestrian was 135 pounds. Using conservation of momentum and the initial speed of the vehicle of 29 mph, the change in speed of the vehicle 0.99 mph. This value compares very favorably with the 1.03 mph ΔV reported by the EDR.

The second step is to model the impact of the pedestrian with the initial speed of the vehicle at 29 mph to determine the throw distance. Using a value of f_p = 0.65, the throw distance s_p is calculated to be 40.6 feet (see Figure 2). The reconstruction with these values shows that the pedestrian was within the crosswalk striping at the time of impact. A check of this solution using one or more Type I models is recommended. In this case, Woods Hybrid Model is used.[27] This model provides the speed of the vehicle for a given throw distance. In this case, the throw distance used in the formula is the value reconstructed using the EDR data: 40.6 feet. This reconstructed throw distance is used with the Wood Hybrid equation to give vehicle speed. This speed can be checked with the speed imaged from the EDR.

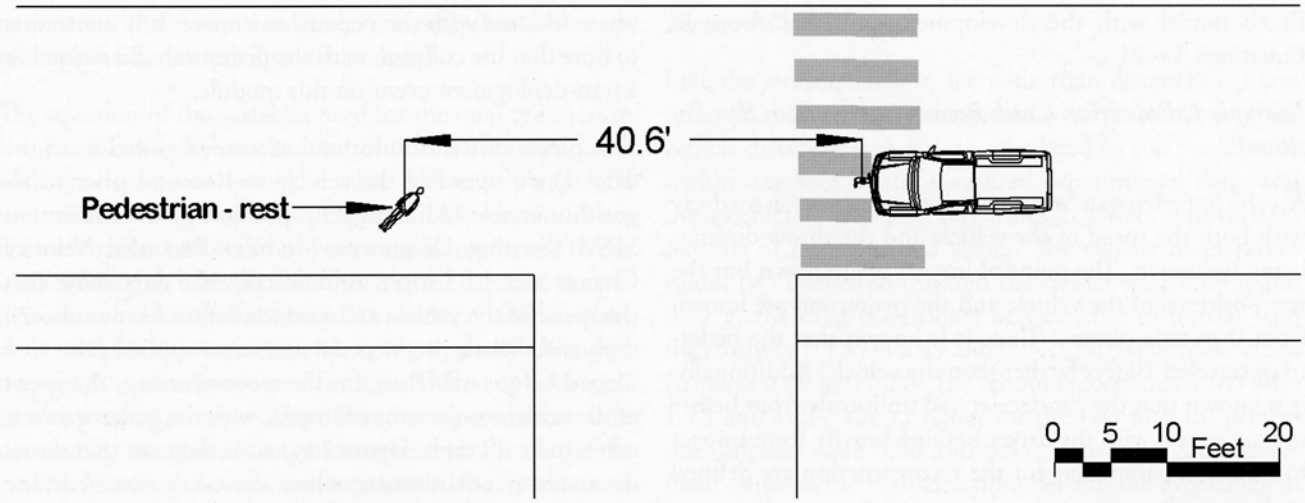

Figure 2: Scale diagram showing the intersection where the crash occurred and the rest position of the pedestrian. One value of the throw distance determined in the reconstruction is also shown

The Wood Hybrid Equation [27] is shown in Equation 13:

$$V_{COL} = c_W \sqrt{s_p} \quad (13)$$

The quantity s_p is the pedestrian throw distance and the parameter c_W is assigned three values comprising a MIN, MAX and mean values for the vehicle speed, V_{COL}. For a throw distance of 40.6 feet, and the three parameter values for c_W presented by Wood, the MIN speed is 19.7 mph, the MAX speed is 35.4 mph, and the mean speed is 28.3 mph. The speed of the vehicle from the EDR data is 29 mph. This EDR speed is in the MIN/MAX range predicted by Equation 13 and differs from the mean value by a little over 2%. This shows that the results using the Type II equation match nicely with this Type I equation. Additional work at this point in the reconstruction might be to examine the effect of the uncertainties in the reconstruction. This work is not presented here.

Example 3: Motorcycle Rider Crash Reconstruction Using Pedestrian Throw Model

This example shows the breadth of the applicability of this Type II model. In this example, a crash involving a motorcycle colliding into the left front wheel of a minivan is reconstructed. Because of the sudden deceleration of the motorcycle to a complete stop, the rider separated from the motorcycle and was projected over the hood of the vehicle, landing on the roadway and tumbling to rest. Figure 3 shows a scale diagram depicting the intersection where the crash occurred with several of the positions of the motorcycle and the rider shown. These positions were measured by the police during their crash investigation. A reconstruction of the crash was needed to determine the speed of the motorcycle at the time of impact and its speed prior to braking.

Before proceeding to the reconstruction of the speed of the motorcycle, consideration of this application of the method is needed. The authors are not aware of any formal treatment of the use of Type I or Type II pedestrian throw models as a method for the reconstruction of the speed of a motorcycle involved in a crash. The notion of the application of a pedestrian throw model applied to a motorcycle rider has been presented previously.[17,26,30] However, while the title of the first paper mentions the application to motorcyclists and mentions it tangentially in the paper, there is no formal consideration of the application separate from the primary topic of the paper which is the application to vehicle/pedestrian impact. The last paper presents a hypothetical example of a motorcycle rider without consideration of the assumptions underpinning the application. One treatment of the subject formally considers a vaulting rider, including data references for the range of launch angle from experimental data and considers the vault of the rider including the vault of a passenger, has been presented by Baxter.[31] The treatment presented here expands on that presented by Baxter by formalizing various of the concepts and utilizing the Han-Brach Type II model rather than a simple vault equation and throw-distance equation.

A necessary requirement for the application of a Type I or Type II model to motorcycle rider projection is that the motorcycle stops suddenly due to the impact and is accompanied by the projecting of the rider from the seat of the motorcycle. In this way, the motion of the rider is consistent with the kinematics and kinetics addressed by Type I and Type II pedestrian throw models. Dynamics of motorcycle/vehicle impacts in which the motorcycle is laid

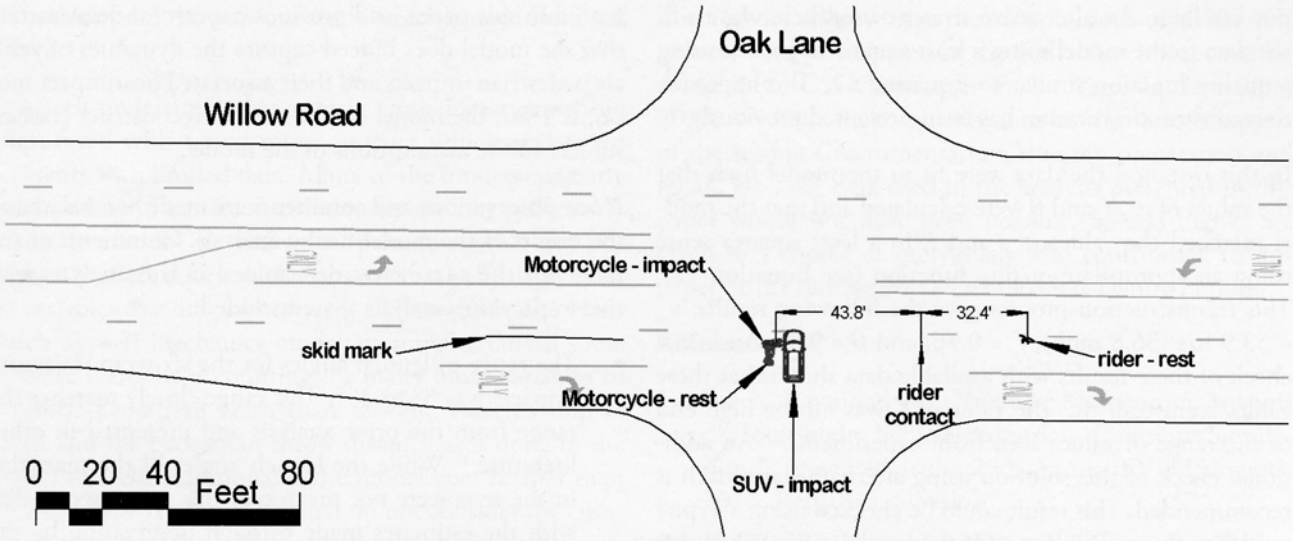

Figure 3: Scale diagram showing the intersection where the crash occurred and various positions relevant to the speed reconstruction

down prior to impact, or the motorcycle swipes the front, side or rear of the vehicle such that the rider is deposited onto the roadway and slides to rest, are not consistent with the application of these models.

A second consideration relative to this application deals with the potential interaction between the rider and the motorcycle and/or the rider and the vehicle as the rider is being projected. Even if the assumption that the rider is projected is met, in general, the reconstructed speed using this application will be a lower bound only. This reconstructed speed is a bound as the model assumes that, as the rider is projected, the initial speed of the motorcycle (prior to impact) is the initial speed of the rider. However, the model does not account for any part of the rider (torso, leg, foot, etc.) interacting with either the motorcycle (fuel tank, handlebars, fairing, etc.) or the vehicle (hood, roof line, fender, etc.). Note that the evidence of this interaction may be very subtle and not readily noticeable to the reconstructionist. Any interaction between the rider and either vehicle would invariably lower the initial speed of the rider (prior to the unimpeded flight) and thus decrease the throw distance. As the reconstructed speed of the rider is the surrogate for the preimpact speed of the motorcycle, the speed of the motorcycle reconstructed using this method serves only as a lower bound; i.e. the actual speed may be higher depending on whether there was interaction or not (which is generally indeterminate). Additionally, it does not appear that this method has been considered in the literature for crashes in which the motorcycle has two riders. Uncertainty therefore exists in the application of this method to crashes with motorcycles involving more than one rider.

In this example, it is assumed that the post-impact motion of the motorcycle rider was consistent with the pedestrian flight motion modeled by the Han-Brach model. The physical evidence from the crash was sufficient to establish the position of the rider at the time of launch and the rest position of the rider. These two locations provided the throw distance, s_p. Using Equation 3, the throw distance is $R + s = s_p$ as x_L is zero in this instance. The physical evidence showed that this distance was 76.2 feet. In addition, the physical evidence also provided the values of the components of the throw distance, R and s. The interaction of the rider and the roadway, primarily due to visible scuffing from the helmet and the clothing, discernably indicated the tumble distance of the rider as 32.4 feet. Thus, the distance R was 43.8 feet (see Figure 3). These values of R and s, along with appropriate values of φ, μ, and α, were sufficient for the application. Here $\varphi = 0.0$ (the roadway was essentially flat and level). The value $\alpha = 1.0$ as the rider was not directly propelled via momentum transfer by an impact from another vehicle and μ was constrained to equal to f_p also based on prior work.[19]

In this application of the Equations 3 through 11, the motion of the vehicle and the momentum exchange was neglected. Only the flight and tumble of the pedestrian (but also including the impact with the pavement and the associated speed change) was used to reconstruct the initial speed of the rider. In addition to the unknown initial speed of the rider, the launch angle, θ, was not known. Moreover, the drag of the pedestrian over the tumble distance s, f_p, was also not known. A traditional strategy to reconstruct under these circumstances is to compute the speed of the motorcycle for appropriate ranges of these in-

put variables. An alternative strategy used here was to fit the data to the model using a least squares approach using a quality function similar to Equation 12. This approach to reconstructing crashes has been presented previously.[24]

In this instance, the data were fit to the model such that the values of v_{c0}, f_p and θ were calculated and that the model matched the values of s and R in a least squares sense using an appropriate quality function (see Equation 12). This reconstruction process gave the following results: v_{c0} = 53.9 ft/s (36.8 mph), f_p = 0.76, and θ = 9.9°. An initial check of these results with available data shows that these values seem realistic. The value of f_p was on the high end of the range of values seen from experiments.[25] An additional check of this solution using alternative approach is recommended. This result could be checked using a Type I model to assess the efficacy of this application. While this process is used frequently by the authors as shown in Example 2, a different approach was used in this situation. In addition to the physical evidence observed on the roadway, the minivan was equipped with an EDR. This EDR was imaged during the vehicle inspection and, in addition to other data, provided a lateral ΔV from the impact with the motorcycle. In this case, the impact between the motorcycle and the minivan was modeled using planar impact mechanics [22] to assess whether the ΔV for the reconstructed impact speed of the motorcycle was close to the value contained in the imaged data. The values were very close, thus providing a second method indicating confidence that the results of the reconstruction are correct.

The reconstruction of the speed at the start of the skid mark (see Figure 3) was also needed. In this case, the mark on the roadway was approximately 41.5 feet long. The mark was attributed to skidding of the rear wheel only. Assuming there was no speed loss of the motorcycle between the end of the skid mark and impact (approximately 44 feet) and that the frictional drag was f = 0.35 for rear wheel braking only, the speed of the motorcycle at the start of the skid mark was 62.4 ft/s (42.6 mph). Any contribution from the front brake over the distance from the start of the skid mark to impact or from the rear brake between the end of the skid mark and impact would increase the speed above the reconstructed value 42.6 mph.

Discussion

The utility of the Han-Brach Type II pedestrian impact model as a reconstruction tool relies on two main points: 1) the ability of the model to capture the kinematics and kinetics of vehicle-pedestrian collisions, and 2) guidance regarding the range of each of the individual empirical parameters. These ranges are needed to apply the model to reliably reconstruct real-world crashes. The analyses presented in this paper, and previous papers [19,21] demonstrate that the model does indeed capture the dynamics of vehicle pedestrian impacts and their associated postimpact motions. Thus, the model can be used to reconstruct crashes, subject to the assumptions of the model.

A few observations and comments are made here related to the results of the model-fitting analysis. Comments of the range for the parameters determined in this analysis relative to previous analysis [19] are included:

- The range of launch angles for the six wrap trajectory impacts was 5° to 25°. This range closely matches the range from the prior analysis and presented in other literature.[31] While the launch angles of the manikins in the tests were not measured, this range agrees well with the estimates made through observation by the authors of the videos.

- The resulting average frictional drag of the pedestrian f_p from the fitting process was f_p = 0.53 with a standard deviation of 0.09. The range consisted of a minimum of 0.38 and a maximum of 0.66. The previous study constrained the value in the fitting process to between 0.7 and 0.8 with the fitting process generally taking on one of the extremes of the range. The parameter was unconstrained in the analysis presented here to assess whether the values produced via the least squares best fit process resulted in a reasonable average value. While the average value of f_p = 0.53 from the analyses here is lower than the constrained range utilized in the previous study, it is consistent with previously published data.[15,25] The resulting range from the data here, $0.38 \le f_p \le 0.66$, is generally lower than the range of $0.55 \le f_p \le 0.9$ reported previously [19] and based on data from another publication.[29] Additional experimental data will help refine the understanding of this parameter and its dependence on factors such as clothing and biofidelity of the manikin.

- In previous studies, the value of μ was assumed to be the same as the pedestrian sliding drag factor, f_p. In this analysis, the value of μ was allowed to vary independent from f_p in the fitting process. This approach was used to gain insight into the behavior of this parameter. In all but one case, the value of μ was greater than the value of f_p. The range of the ratio μ/f_p is 0.9 to 2.2 with an average of 1.5 and a standard deviation of 0.5.

- The value of α was kept at 1.0 for the wrap trajectory trials, consistent with the previous analysis.[19] It was allowed to vary for the two forward projection trials. The two values for the parameter from the two trials were 1.3 and 1.1. These values are consistent with the

values from the previous study which ranged from 1.2 to 1.3.[19]

It is well-understood that vehicle crash investigators are often faced with trying to reconstruct vehicle-pedestrian accidents with limited data. Many of the models currently employed by these reconstructionists are not sufficiently robust to account for individual parameters that can significantly affect their calculations or are wholly dependent on variables that are unknown for a given crash. The Han-Brach Type II mechanics model attempts to curtail some of those issues by accounting for many more variables in a vehicle-pedestrian crash than just the vehicle's impact speed and the pedestrian throw distance as is done in the Type I models. Additionally, the model goes further than previous Type II models [18,26] that do not consider the combined motion of the vehicle and the pedestrian or does not include the impacts (vehicle-pedestrian and/or pedestrian-roadway) in the development. The purpose of the current research was to further validate the Han-Brach model with a detailed data set of realistic vehicle-pedestrian impacts.

The application of the Han-Brach model to the ARC-CSI vehicle-pedestrian impact test data was a successful demonstration of the model's ability to accurately reflect real-world data. The modeled data matched extremely well with highly reliable, measured data. The analysis provided refined ranges for several other parameters such as vehicle deceleration, drag coefficients, and pedestrian launch angles that are often unknown and/or difficult to measure directly in testing. The ability to use these values along with known physical evidence and reasonable estimates of other parameters provides users with a powerful, reliable tool to perform accurate reconstructions of vehicle-pedestrian crashes. This utility was further demonstrated with the examples of real-world accident reconstructions.

It should be recognized that not all vehicle-pedestrian impacts can be effectively reconstructed with Type II models such as the Han-Brach model. A prime example of this is when the specific movements of the pedestrian need to be modeled. In these situations, users may wish to pursue Type III models when appropriate. Type I models, which generally require the user to know the throw distance, provide utility in checking the reconstruction results of Type II and Type III models. Lastly, the authors encourage other researchers to further study the Han-Brach model by employing different combinations of pedestrian dimensions, impact speeds and orientations, and braking responses. Additional well-documented experimental data for the value of f_p, under various conditions, will assist in the application of this method.

Acknowledgments

The authors acknowledge the contributions of all the volunteers who participated in the pedestrian impact testing at the ARC-CSI Conference in Las Vegas in September 2017. Without their contributions to the various aspects of the testing (instrumentation, dummy preparation and repair, etc.) the data used in the analysis presented in this paper would not have been possible. Special thanks are given to a couple of individuals who contributed to this paper or the testing: Mike DiTallo, and Danny Phillips.

References

1. Brach, Raymond M., "Impulse-Momentum Analysis of Multibody Vehicle-Pedestrian Collision Simulations", presented at the 25th Annual EVU Congress, 2016, Bratislava, Slovakia.
2. Ravani, B., Brougham, D., and Mason, R., "Pedestrian Post-Impact Kinematics and Injury Patterns," SAE Technical Paper 811024, 1981, https://doi.org/10.4271/811024.
3. Happer, A., Araszewski, M., Toor, A., Overgaard, R. et al., "Comprehensive Analysis Method for Vehicle/Pedestrian Collisions," SAE Technical Paper 2000-01-0846, 2000, https://doi.org/10.4271/2000-01-0846.
4. Toor, A., Araszewski, M., Johal, R., Overgaard, R. et al., "Revision and Validation of Vehicle/Pedestrian Collision Analysis Method," SAE Technical Paper 2002-01-0550, 2002, https://doi.org/10.4271/2002-01-0550.
5. Toor, A. and Araszewski, M., "Theoretical vs. Empirical Solutions for Vehicle/Pedestrian Collisions," SAE Technical Paper 2003-01-0883, 2003, https://doi.org/10.4271/2003-01-0883.
6. Russell, Gregory, Pedestrian Formulas for Excel, Lawyers and Judges Publishing Company, Inc.
7. MADYMO, https://tass.plm.automation.siemens.com/madymo
8. PC-Crash, http://www.pc-crash.com/
9. Engineering Dynamics Corporation, http://www.edccorp.com/products/gatb.html
10. Hamacher, M., L. Eckstein and R. Paas, "Vehicle Related Influence of Post-Car Impact Pedestrian Kinematics on Secondary Impact", IRC-12-78, IRCOBI Conference 2012.
11. Moser, A., Steffan, H., and Kasanický, G., "The Pedestrian Model in PC-Crash - The Introduction of a Multi Body System and its Validation," SAE Technical Paper 1999-01-0445, 1999, https://doi.org/10.4271/1999-01-0445.
12. Moser, A., Hoschopf, H., Steffan, H., and Kasanický, G., "Validation of the PC-Crash Pedestrian Model,"

SAE Technical Paper 2000-01-0847, 2000, https://doi.org/10.4271/2000-01-0847.

13. Day, T., "An Overview of the HVE Human Model," SAE Technical Paper 950659, 1995, https://doi.org/10.4271/950659.
14. Depriester, J-P, C. Perrin, T. Serre, S. Chalandon, "Comparison of Several Methods for Real Pedestrian Accident Reconstruction," Proc. Int. Tech. Conf. Enhanced Safety Vehicles 2005; 14p.
15. Stevenson, T. J., Simulation of Vehicle-Pedestrian Interaction, doctoral dissertation, 2006, https://ir.canterbury.ac.nz/handle/10092/1180.
16. Collins, J. C., Accident Reconstruction, Charles C. Thomas, Springfield, IL, 1979.
17. Searle, J. and Searle, A., "The Trajectories of Pedestrians, Motorcycles, Motorcyclists, etc., Following a Road Accident," SAE Technical Paper 831622, 1983, https://doi.org/10.4271/831622.
18. Searle, J., "The Physics of Throw Distance in Accident Reconstruction," SAE Technical Paper 930659, 1993, https://doi.org/10.4271/930659.
19. Han, Inhwan and Raymond M. Brach, "Throw Model for Frontal Pedestrian Collisions," SAE Technical Paper 2001-01-0898, 2001, https://doi.org/10.4271/2001-01-0898.
20. Evans, A.K. and R. Smith, "Vehicle speed calculation from pedestrian throw distance," IMechE, Proc Instn Mech Engrs, Vol 213, Prt D, 1999.
21. Brach, Raymond M., "Reconstruction of Vehicle-Pedestrian Collisions Including an Unknown Point of Impact," SAE Technical Paper 2015-01-1419, 2015, https://doi.org/10.4271/2015-01-1419.
22. Brach, Raymond M. and R. Matthew Brach, Vehicle Accident Analysis and Reconstruction Methods, 2nd Edition, Publication R-397, SAE International, Warrendale, PA, 2011.
23. Kazanický, Gustav and Pavol Kohút, New Partial Overlap Pedestrian Impact Tests, presented at the 18th Annual EVU Congress, Hinckley (UK), 2009.
24. Brach, R. Matthew, Brach, Raymond M., and Mink, Richard, "Nonlinear Optimization in Vehicular Crash Reconstruction," SAE Int. J. Trans. Safety 3(1):17-27, 2015, https://doi.org/10.4271/2015-01-1433.
25. Wood, Denis, and Ciaran Simms, Coefficient of Friction in Pedestrian Throw, Impact – Journal of ATAI, vol 9 no 1, p12-14, January 2000.
26. Aronberg, R., "Airborne Trajectory Analysis Derivation for Use in Accident Reconstruction," SAE Technical Paper 900367, 1990, https://doi.org/10.4271/900367.
27. Wood, Denis P. and C. K. Simms, (2000) A hybrid model for pedestrian impact and projection, International Journal of Crashworthiness, 5:4, 393-404, DOI: 10.1533/cras.2000.0150.
28. Aronberg, R. and Snider, A., "Reconstruction of Automobile/Pedestrian Accidents Using CATAPULT," SAE Technical Paper 940924, 1994, https://doi.org/10.4271/940924.
29. Hill, G. S., Calculations of Vehicle Speed from Pedestrian Throw, Impact, J. Inst. Traffic Accident Investigation, Spring 1994.
30. Obenski, Kenneth S., et al., Motorcycle Accident Reconstruction and Litigation, Lawyers and Judges Publishing Company, Inc. Tucson, AZ, 2011.
31. Baxter, Albert T., Motorcycle Accident Investigation, 2nd Edition (revised), Institute of Police Technology and Management, Jacksonville, Florida, 1997.

Appendix A

Previously presented in this paper is the equation for the speed change along the roadway (ΔV_x) of the pedestrian due to the impact between the pedestrian and the roadway. This speed change is needed so that the velocity of the pedestrian along the roadway at the start of the slide distance can be calculated. That equation is:

$$v'_{pRx} = v_{pRx} + \mu v_{pRy} \tag{A.1}$$

The form of this equation may seem rather terse and its source not obvious. As will be shown here, it follows directly from point mass impact dynamics.[22] The equations for the velocity change in the tangential direction for mass 1 of a collision involving two point masses is:

$$V_{1t} = v_{1t} + \mu \frac{\bar{m}}{m_1}(1+e)(v_{2n} - v_{1n}) \tag{A.2}$$

Where: $\bar{m} = \dfrac{m_1 m_2}{m_1 + m_2}$.

In this case, m_2 is the roadway, i.e. the earth. Thus, $m_2 \approx \infty$ and $v_{2n} = 0$. Moreover, the value of $\bar{m}$ can be found using the equation above and the notion of a limit for $m_2 \to \infty$. This gives the result that $\bar{m} = m_1$. Going back to Equation A.2 with $v_{2n} = 0$ and $\bar{m} = m_1$, and that the assumption here is the impact is inelastic ($e = 0$, no rebound), Equation A.2 becomes:

$$V_{1t} = v_{1t} + \mu(-v_{1n}) \tag{A.3}$$

This equation has the same form as Equation 10 (repeated in Equation A.1).

Appendix B

	S4	S8	M4	M5	M6	M7	S2a	S3
Input Information (Knowns)								
	Wrap Trajectory						**Forward Proj**	
a_0	0.805	0.719	0.747	0.668	0.638	0.680	0.706	0.689
a_2	0.805	0.719	0.747	0.668	0.638	0.680	0.706	0.689
f_p	0.517	0.548	0.528	0.383	0.664	0.463	0.486	0.638
g (ft/s^2)	32.174	32.174	32.174	32.174	32.174	32.174	32.174	32.174
h (ft)	5.000	3.500	3.330	5.000	2.000	3.250	3.000	2.333
s_1	0.000	0.000	0.000	0.000	0.000	0.000	0.000	0.000
v_{c0} (ft/s)	50.160	49.867	49.779	47.667	46.200	50.893	41.844	46.875
v_{c0} (mph)	34.200	34.000	33.940	32.500	31.500	34.700	28.530	31.960
x_L	10.000	5.000	6.000	10.000	5.000	5.000	9.000	7.500
α	1.000	1.000	1.000	1.000	1.000	1.000	1.281	1.145
θ	25.075	15.996	14.957	25.075	4.998	14.485	0.000	0.000
φ	0.000	0.000	0.000	0.000	0.000	0.000	0.000	0.000
μ	0.635	0.684	0.941	0.793	0.592	0.999	0.786	0.797
m_c	121.029	86.871	95.077	83.919	82.054	82.054	154.068	114.533
m_p	4.600	1.834	5.253	4.724	0.684	4.724	4.600	0.684
s_0	14.000	7.000	8.000	13.500	5.000	7.500	8.000	7.500
Output Information (Unknowns)								
v''_{c0}	40.764	45.544	43.356	38.936	43.558	44.970	36.167	42.927
v_{p0}	40.764	45.544	43.356	38.936	43.558	44.970	46.313	49.143
R	32.893	43.700	38.556	44.804	21.252	40.015	20.000	18.716
t_{p1}	1.122	1.143	1.088	1.574	0.601	1.071	0.634	0.547
s	23.407	26.200	17.744	10.296	30.848	21.385	40.100	37.784
s_p	66.300	74.900	62.300	65.100	57.100	66.400	69.100	64.000
t_p	2.800	2.867	2.533	2.867	2.300	2.767	2.900	2.467
t_{c1}	0.303	0.145	0.167	0.304	0.111	0.152	0.202	0.167
s_2	32.061	44.829	39.086	35.253	46.189	46.202	28.778	41.576
$s_0+s_1+s_2$	46.061	51.829	47.086	48.753	51.189	53.702	36.778	49.078
t_c	1.936	2.155	2.070	2.217	2.249	2.325	1.841	2.115
d	-20.239	-23.071	-15.214	-16.347	-5.911	-12.698	-32.322	-14.922
t_0	0.303	0.145	0.167	0.304	0.111	0.152	0.202	0.167
Calculated Parameter Values								
s_p	66.300	74.900	62.300	65.100	57.100	66.400	69.100	64.000
$s_0+s_1+s_2$	46.500	52.200	47.400	49.300	51.700	54.400	37.100	49.000
t_p	2.800	2.867	2.533	2.867	2.300	2.767	2.900	2.467
t_c	1.833	2.067	2.000	2.100	2.133	2.167	1.778	2.133
Q	1.238	0.925	0.590	1.664	1.690	3.009	0.506	0.039

C